Electronic Supplementary Material (ESI) for Journal of Materials Chemistry C.

Supporting Information for

Piperidine Switches on Direct Band Gaps of Ag(I)/Bi(III) Bimetallic Iodide Double Perovskites

Mohamed Saber Lassoued, [a] *Le-Yu Bi,* [a] *Zhaoxin Wu,* [b,c] *Guijiang Zhou,* [d] *and Yan-Zhen Zheng** [a]

---

a *M. S. Lassoued, L.-Y. Bi, Y.-Z. Zheng*

Frontier Institute of Science and Technology (FIST), State Key Laboratory for Mechanical Behavior of Materials, MOE Key Laboratory for Nonequilibrium Synthesis and Modulation of Condensed Matter, Xi'an Key Laboratory of Sustainable Energy and Materials Chemistry, and School of Science, Xi'an Jiaotong University, Xi'an 710049, China.
E-mail: zheng.yanzhen@xjtu.edu.cn

b,c *Z. Wu*

Key Laboratory of Photonics Technology for Information, Key Laboratory for Physical Electronics and Devices of the Ministry of Education, Department of Electronic Science and Technology, School of Electronic and Information Engineering, Xi'an Jiaotong University, Xi'an, China d.Collaborative Innovation Center of Extreme Optics, Shanxi University, Taiyuan 030006, China.

d *G. Zhou*

Ministry of Education Key Laboratory for Nonequilibrium Synthesis and Modulation of Condensed Matter and Department of Chemistry, Faculty of Science, Xi'an Jiao Tong University, Xi'an 710049, P. R. China

Table of Contents

1. Experimental Section

1.1. General remarks

Single crystal X-ray diffraction data of **1** and **2** were recorded on a Bruker detector diffractometer with graphite monochromated Mok radiation (λ= 0.71073 Å) at 150K. PXRD intensities were measured at room temperature on a Rigaku D/max-IIIA diffractometer (Cu-kλ, λ=1.54056 Å). The crystalline powder samples were prepared by grinding the single crystals and collected in the 2Θ range of 5 to 50° at a rate of 10 °/min to determine the purity and the phase identity. TGA experiments were performed on a TGA-50 (SHIMADZU) thermogravimetric analyzer. The ac impedance spectroscopies were conducted on the Metrohm Autolab B.V. PGSTAT204 in the frequency range from 1 to 1 MHz with amplitude of 50 mV and in a humidity range of 30% to 90% at 95 °C. Scanning electron microscopy (SEM) was performed using KYKY-EM3200, 25 KV instrument. Solid-state UV-Vis diffusion reflectance spectra of pressed powder samples were measured on a SHIMADZU UV-3600 UV-Vis-NIR spectrophotometer using $BaSO_4$ powder as the reflectance reference. Room-temperature steady-state emission spectra were collected on powder samples using an Edinburgh FLS9 fluorimeter upon 450 nm excitation. All density-functional theory (DFT) calculations were carried out within the Materials Studio. The Photo response measurement was calculated using a picoammeter (Keithley 6485) in series with a source meter (Keithley 2400) to detect the small current in this test. A 350 W solar-simulating Xenon lamp was used as light source.

2. Materials and Sample Preparation

2.1. Materials

Chemicals listed were used as purchased and without further purification: (i) 4-aminomethylpiperidine, 98%, Alfa Aesar; (ii) 4-aminopiperidine, 98%, sigma Aldrich; (iii) hydroiodic acid, 57% w/w, sigma Aldrich; (iv) bismuth iodide, 99.9 %, sigma Aldrich; (v) silver iodide, 99%, Fisher Scientific

2.2. Preparation of $(AMP)_4[BiAgI_8]_2.H_2O$ and $(APP)_4[BiAgI_8].H_2O$ Single crystals

Red plate crystals of $(C_6H_{16}N_2)_4[BiAgI_8]_2.H_2O$ (**1**) were synthesized from a reaction mixture containing 4-aminomethylpiperidine (0.456 g, 4 mmol), BiI_3 (1.178 g, 2 mmol) and AgI (0.468 g, 2 mmol) in 15 mL of hydrogeniodide acid (HI, 57%), then the mixture was loaded into a 28 mL Teflon-lined stainless steel autoclave. The container was closed and heated at 120 °C for

72 hours. At a rate of 5 °C/h, the system was allowed to cool to room temperature. The crystals of **1** were washed with diethyl ether and dried in vacuum (Yield: *ca*. 71% based on Bi).

Red needle crystals of $(C_5H_{13}N_2)_4[BiAgI_8].H_2O$ (**2**) were obtained from a similar method. A mixture of 4-aminopipyridine (0.4 g, 4 mmol), BiI_3 (0.589 g, 1 mmol) and AgI (0.234 g, 1 mmol) were added to a 15 mL of HI (57%), then the reaction was heated at 120 °C for 3 days. The system was allowed to cool to room temperature at the rate of 5 °C/h. The crystals of **2** were washed with diethyl ether and dried in vacuum (Yield: *ca*. 78% based on Bi).

2.3. Fabrication of $(AMP)_4[BiAgI_8]_2.H_2O$ and $(APP)_4[BiAgI_8].H_2O$ Thin Films

$(AMP)_4[BiAgI_8]_2.H_2O$ and $(APP)_4[BiAgI_8].H_2O$perovskite compounds (0.4 g) were dissolved in 1 mL of DMF solution and were coated onto ITO glass substrate by spin coating technique at 1000 rpm for 60 second. To evaporate the residual solvent, the obtained film was followed by annealing on a hot plate at 70 °C for 10 minutes, visible color change from light red to dark red can be observed.

3. Characterization methods and Simulation details

3.1. Characterization methods

X-ray Crystallographic Study .The structures were solved by direct methods and refined with a full-matrix least-squares technique within the SHELXTL program package.[1] All non-hydrogen atoms were subjected to anisotropic refinement by full-matrix least-squares refinement on F2 using SHELXTL. The crystallographic details are provided in **Table S1–S5**. Crystallographic data for the structural analyses have been deposited at the Cambridge Crystallographic Data Centre. The crystallographic data for above compound can be found in the Supporting Information or can be obtained free of charge from the Cambridge Crystallographic Data Centre via http:**//www.ccdc.cam.ac.uk/data_request/cif**. CCDC Numbers: 1975061 (**1**), 1975058 (**2**).

Proton conductivity measurements. The two sample were pressed into a cylinder pellet of crystalline powder sample by transferring to a standard 13 mm die and pressed with 15 MPa for 10 munites (13 mm diameter* 0.5 mm to 1 mm thickness for **1** and **2**) coated with silver colloid. The pellet was connected to two Pt wires at both sides using conductive silver paste and then the four electrodes are linked to the two Pt wires. It's important to note that the silver paste must cover the measurement area (Sheme S1). The proton conductivity was estimated by semi cercle fitting of Nyquist plots.

A : Reference electrode 1

B : Working electrode

C : Reference electrode 2

D : Counter electrode

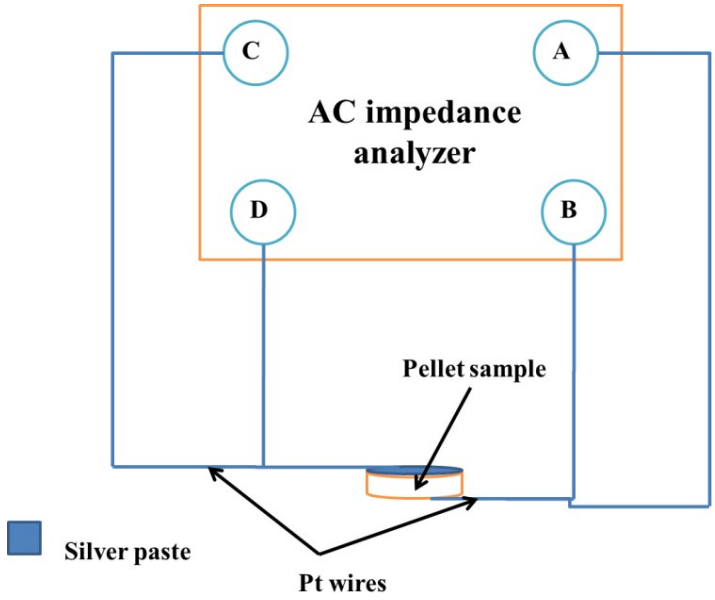

Scheme S1. A diagram showing quasi-four-probe method (also called two-probe method) for proton conductivity measurement.

TG analysis. TG analysis experiment of **1** and **2** polycrystalline powder were performed with a heating rate of 10 °C min^{-1} under N_2 atmosphere from 30 to 600 °C under nitrogen gas atmosphere. The weight loss of these two compound began from 290 °C and 285 °C for **1** and **2** respectively due to the degradation of the organic part.

UV-vis-NIR Diffuse Reflectance Spectroscopy. The $BaSO_4$ powder sample was used as a reference (100% reflectance) and Absorption (K/S) data were calculated from the following Kubelka-Munk function: $K/S = (1–R)^2/2R$, where R is the reflectance, K is the absorption, and S is the scattering.

Photoluminescence measurement. Room-temperature steady-state emission spectra were collected on powder samples upon 450 nm excitation. The CIE chromaticity coordinates, CRI color rendering index and CCT correlated color temperatures were calculated using the OSRAM Company's Color Calculator software available from **https://www.osram-americas.com**.

Photo response measurement. The pellets were prepared by grinding 50-100 mg polycrystalline samples of **1** and **2** into a homogeneous powder after pressed with 15 MPa for 10 minutes. Each pellet was connected to two wires at one side (up or down) using conductive silver paste. It's worthy to note that we left one narrow strip like area without paint which can receive light from the lamp. A 350 W solar-simulating Xenon lamp was used as light source. For each 40 s we past or blocked the light and detected the current change.

The on/off ratio of the photodetector is calculated using equation **1**.

$$\text{ON /OFF} = I_{light} / I_{dark} \textbf{(1)}$$

Where I_{light} is the photocurrent (79.31 nA for **1** and 56.01 nA for **2**) and I_{dark} is the dark current (5.64 nA and 2.80 nA for **1** and **2** respectively).

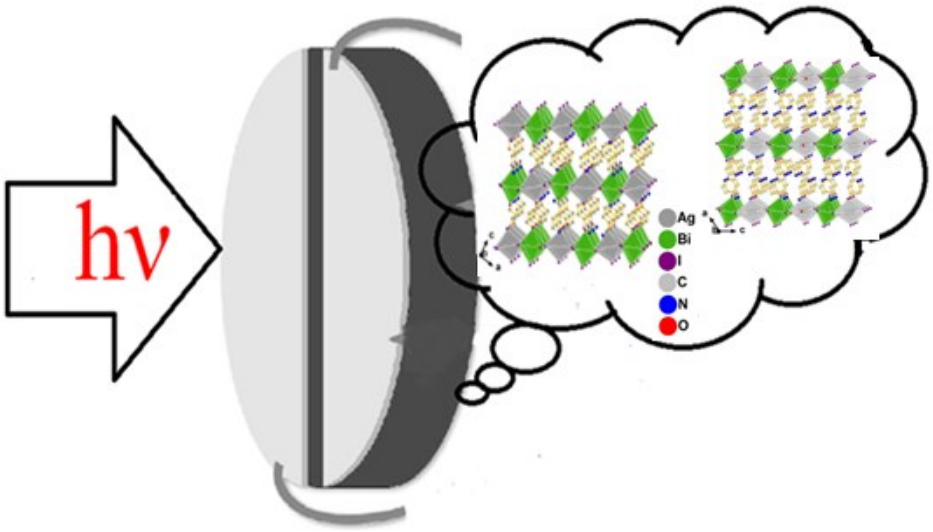

Sheme S2. Scheme of photo-response test device.

Stability studies. Freshly prepared powder samples and films of **1** and **2** were stored either in the dark to minimize light exposure and the relative humidity was maintained at ~55% humidity for 30 days.

3.2. Simulation details

The First-principles density functional theory (DFT) [2] calculations were performed in the framework of the CASTEP [3] (Cambridge Serial Total Energy Package) module of Materials Studio 2017 in an elastic compute servicer with 24 cores and 96 GB memory. The functional developed by Ceperley and Alder data as parameterized by Perdew and Zunger (CA-PZ) in the framework of the local density approximation (LDA) [4] form was adopted to describe the exchange correlation energy. The equilibrium crystal structures were achieved by utilizing geometry optimization. The convergence threshold for the self-consistent field was 10^{-6} Ha. The other parameters and convergent criteria were the default values of CASTEP code. When excluding the spin orbit coupling (SOC), the kinetic energy cutoff we used was 260 eV with ultrasoft pseudopotentials. For the case of including the SOC, we applied norm-conserving pseudo potentials [5] in the Kleinman Bylander [6] form for all the elements were used to model the effective interaction between atom cores and valence electrons. With SOC, our approach

gives rather small difference between theory and experiment for lattice constants, and provides correct trends of band gap values and shows good experiment–theory agreement of gap values.

4. Supporting Tables and Figures

Table S1 Summary of crystal data and structural refinements of **1** and **2**

	1	**2**
CCDC number	1975061	1975058
Empirical formula	$C_{24}H_{66}Bi_2Ag_2I_{16}N_8O$	$C_{20}H_{54}BiAgI_8N_8O$
Formula weight	3146.95	1754.76
Crystal dimensions (mm)	0.12*0.2*0.14	0.13*0.18*0.11
Crystal system	Monoclinic	Monoclinic
Space group	C2/c	C2/c
a/Å	34.882(14)	32.576(9)
b/Å	8.442(4)	8.589(2)
c/Å	22.114(9)	19.604(5)
α/°	90	90
β/°	97.105(5)	125.138(3)
γ/°	90	90
Volume/Å^3	6462(5)	4486(2)
Z	4	4
ρ calcg/cm^3	3.235	2.598
μ /mm^{-1}	13.699	9.884
F(000)	5528.0	3168.0
Index ranges	-44<=h<=44, -10<=k<=10, -28<=l<=28	-38<=h<=38, -10<=k<=10, -23<=l<=23
Reflections collected	37617	24174
Data Completeness	98.7%	99.9%
Data/restraints/parameters	7958/0/484	3939/1/193
Goodness-of-fit on F2	1.082	1.059
Weight	w = 1/[σ2(Fo2) + (0.0151P)2 + 209.7691P]where P = (Fo2 + 2Fc2)/3	w = 1/[σ2(Fo2) + (0.0397P)2 + 18.8185P] where P = (Fo2 + 2Fc2)/3
R=∑||Fo−Fc||/∑|Fo|,wR	R_1 = 0.0387, wR_2 = 0.0886	R_1 = 0.0368, wR_2 = 0.091

$R1 = \Sigma||Fo| - |Fc||/\Sigma|Fo|$, $wR_2 = [\Sigma w(Fo^2 - Fc^2)^2 / \Sigma w(Fo^2)^2]^{1/2}$

Table S2 Summary of selected bond lengths (Å) and bond angles (°) of **1**.

Bond	Lengths/Å	Bond pair	Angles / °
Bi1-I1	3.1090 (11)	I5-Bi1-I6	92.93 (3)
Bi1-I2	3.1897 (11)	I5-Bi1-I4	93.35 (4)
Bi1-I3	3.2118 (13)	I6-Bi1-I4	89.16 (2)
Bi1-I4	3.0436 (11)	I5-Bi1-I1	89.93 (4)
Bi1-I5	2.9849 (10)	I6-Bi1-I1	89.98 (2)
Bi1-I6	2.9955 (12)	I4-Bi1-I1	176.643 (19)
Ag1-I7	2.7322 (10)	I5-Bi1-I2	176.590 (18)
Ag1-I2	3.3349 (10)	I6-Bi1-I2	88.21 (3)
Ag2-I5	3.3256 (13)	I4-Bi1-I2	89.88 (3)
Ag2-I8	2.6663 (11)	I1-Bi1-I2	86.85 (3)
Ag1-I7i	2.7322 (10)	I5-Bi1-I3	93.04 (3)
Ag2-I8ii	2.6663 (11)	I6-Bi1-I3	173.657 (18)
N3-C7	1.504 (11)	I4-Bi1-I3	88.34 (2)
N1-C1	1.494 (11)	I1-Bi1-I3	92.19 (2)
C8-C12	1.517 (12)	I2-Bi1-I3	85.96 (3)
C7-C8	1.517 (12)	Bi1-I2-Ag1	163.40 (2)
C8-C9	1.538 (13)	Bi1-I5-Ag2	177.50 (2)
N2-C4	1.493 (12)	I7i-Ag1-I7	180.000 (16)
N2-C5	1.506 (12)	I7i-Ag1-I2	92.24 (3)
C9-C10	1.509 (13)	I7-Ag1-I2	87.76 (3)
C1-C2	1.505 (12)	I8-Ag2-I8ii	170.24 (6)
C2-C3	1.515 (12)	I8-Ag2-I5	93.41 (3)
C2-C6	1.536 (12)	I8ii-Ag2-I5	92.66 (3)
N4-C10	1.504 (12)	C10-N4-C11	113.5 (8)
N4-C11	1.507 (13)	N3-C7-C8	111.6 (7)
C5-C6	1.517 (14)	N4-C10-C9	110.6 (8)
C11-C12	1.515 (14)	N2-C5-C6	109.7 (8)
C3-C4	1.512 (15)	C12-C8-C7	108.2 (8)
		C12-C8-C9	109.1 (7)
		C7-C8-C9	113.8 (7)
		C4-N2-C5	111.8 (7)
		C10-C9-C8	112.4 (8)
		C1-C2-C3	110.1 (7)
		C1-C2-C6	112.8 (8)
		C3-C2-C6	108.5 (8)
		C11-C12-C8	112.3 (9)
		C5-C6-C2	112.0 (8)
		C2-C3-C4	112.6 (8)
		N1-C1-C2	113.1 (7)
		N4-C11-C12	109.6 (7)
		N2-C4-C3	110.3 (9)

Symmetry codes: (i) −x + 1/2, −y+1/2, −z+1; (ii) −x + 1, y, −z + 3/2.

Table S3 Summary of selected bond lengths (Å) and bond angles (°) of **2**.

Bond	Lengths/Å	Bond pair	Angles / °	Bond pair	Angles / °
Ag1-Ag1A	0.692 (10)	Ag1A-Ag1-Ag1Ai	137 (4)	C2-C3-N2	111.0 (8)
Ag1-Ag1Ai	0.692 (10)	Ag1Ai-Ag1-I1i	84.0 (15)	N2-C3-C4	109.7 (7)
Ag1-I1	2.6928 (12)	Ag1Ai-Ag1-I1	89.2 (14)	C3-C4-C5	109.9 (9)
Ag1-I1i	2.6928 (12)	Ag1A-Ag1-I1i	89.2 (14)	C4-C5-N1	111.1 (9)
Ag1-I2	3.212 (3)	Ag1A-Ag1-I1	84.0 (15)	C7-C6-N3	110.1 (9)
Ag1-I2i	3.212 (3)	Ag1Ai-Ag1-I2i	61.0 (19)	C6-C7-C8	110.3 (8)
Ag1A-Ag1Ai	1.29 (3)	Ag1Ai-Ag1-I2	162 (2)	C9-C8-C7	112.7 (8)
Ag1A-I1	2.709 (18)	Ag1A-Ag1-I2	61.0 (19)	C9-C8-N4	110.7 (7)
Ag1A-I1i	2.771 (17)	Ag1A-Ag1-I2i	162 (2)	N4-C8-C7	108.6 (8)
Ag1A-I2	2.94 (2)	I1i-Ag1-I1	161.28 (18)	C8-C9-C10	109.8 (8)
Ag1A-I3ii	3.229 (9)	i1-Ag1-I2i	99.33 (6)	N3-C10-C9	110.1 (9)
Bi1-I2iii	3.0754 (8)	I1-Ag1-I2	92.59 (5)	C5-N1-C1	110.2 (10)
Bi1-I2	3.0754 (8)	I1i-Ag1-I2	99.33 (6)	C6-N3-C10	112.6 (9)
Bi1-I3	3.0727 (8)	I1i-Ag1-I2i	92.59 (5)		
Bi1-I3iii	3.0727 (8)	I2i-Ag1-I2	100.81 (12)		
Bi1-I4iii	3.1054 (10)	Ag1-Ag1A-Ag1Ai	21 (2)		
Bi1-I4	3.1054 (10)	Ag1-Ag1A-I1	81.3 (15)		
Ag1Ai-I1	2.771 (17)	Ag1-Ag1A-I1i	76.3 (14)		
Ag1Aii-I3	3.229 (9)	Ag1-Ag1A-I2	107 (2)		
C1-C2	1.511 (14)	Ag1-Ag1A-I3ii	164 (2)		
C1-N1	1.532 (15)	Ag1Ai-Ag1A-I1i	73.7 (15)		
C2-C3	1.504 (14)	Ag1Ai-Ag1A-I1	79.1 (15)		
C3-C4	1.515 (14)	Ag1Ai-Ag1A-I2	128.50 (17)		
C3-N2	1.507 (12)	Ag1Ai-Ag1A-I3ii	142.6 (4)		
C4-C5	1.523 (14)	I1-Ag1-I1i	151.7 (7)		
C5-N1	1.530 (14)	I1i-Ag1-I2	104.4 (6)		
C6-C7	1.509 (14)	I1-Ag1A-I2	98.6 (6)		
C6-N3	1.514 (15)	I1-Ag1A-I3ii	100.5 (4)		
C7-C8	1.534 (14)	I1i-Ag1A-I3ii	96.4 (4)		
C8-C9	1.495 (13)	I2-Ag1A-I3ii	88.8 (4)		
C8-N4	1.518 (12)	I2iii-Bi1-I2	180.0		
C9-C10	1.524 (13)	I2-Bi1-I4	87.35 (2)		
C10-N3	1.522 (14)	I2iii-Bi1-I4	92.65 (2)		

Symmetry codes: (i) -x + 1, y, -z + 1/2; (ii)-x + 1, -y + 1, -z + 1; (iii) -x + 1, -y, -z + 1

Table S4 Hydrogen bonding data of compound **1**

D-H	d(D-H)	d(H..A)	<DHA	d(D..A)	A
O1-H1F	0.850	2.727	172.73	3.572	I4(a)
O1-H1G	0.850	2.322	124.17	2.886	N2
O1-H1G	0.850	3.211	127.54	3.790	I5(b)
O1-H1G	0.850	3.326	117.14	3.790	I5(c)
N3-H3A	0.890	2.718	162.72	3.577	I7(d)
N3-H3B	0.890	2.699	161.91	3.556	I3
N3-H3C	0.890	2.910	136.99	3.612	I2
N3-H3C	0.890	3.223	114.41	3.681	I1
N1-H1A	0.890	2.747	165.20	3.615	I7(e)
N1-H1B	0.890	2.804	174.55	3.691	I3
N1-H1C	0.890	3.027	134.82	3.709	I1(f)
N1-H1C	0.890	3.175	114.49	3.635	I4
N2-H2A	0.900	2.778	177.22	3.677	I8(g)
N2-H2B	0.900	2.035	157.37	2.886	O1
N2-H2B	0.900	3.319	113.08	3.764	I5(h)
N4-H4A	0.900	2.777	160.86	3.639	I6(i)
N4-H4B	0.900	2.873	145.22	3.649	I1(j)

Symmetry transformations used to generate equivalent atoms : (a) [-x + 1, -y + 1, -z + 1] ; (b) [-x + 1, -y + 1, -z + 1] ; (c) [x, -y + 1, z - 1/2] ; (d) [-x + 1/2, -y + 3/2, -z + 1] ; (e) [-x + 1/2, -y + 1/2, -z + 1] ; (f) [x, y - 1, z] ; (g) [x, -y + 1, z - 1/2] ; (h) [-x + 1, -y + 1, -z + 1] ; (i) [x, -y + 1, z - 1/2] ; (j) [x, -y + 2, z-1/2]

Table S5 Hydrogen bonding data of compound **2**

D-H	d(D-H)	d(H..A)	<DHA	d(D..A)	A
N2-H2C	0.910	2.908	133.40	3.594	I3(a)
N2-H2C	0.910	3.195	119.89	3.733	I3(b)
N2-H2D	0.910	2.717	171.01	3.618	I1
N2-H2E	0.910	2.791	167.04	3.684	I4(c)
N4-H4C	0.910	2.972	156.78	3.825	I1(d)
N4-H4C	0.910	3.306	116.12	3.796	I2(e)
N4-H4D	0.910	2.918	161.07	3.790	I4(f)
N4-H4E	0.910	1.979	167.84	2.875	O1
O1-H1C	0.850	2.696	167.82	3.532	I3
O1-H1D	0.850	2.154	142.38	2.875	N4(g)

Symmetry transformations used to generate equivalent atoms : (a) [x, -y + 1, z - 1/2]; (b) [-x + 1, y, -z + 1/2]; (c) [-x + 1, y, -z + 1/2]; (d) [-x + 1, -y, -z + 1]; (e) [-x + 1, -y, -z + 1]; (f) [x, -y, z + 1/2]; (g) [-x + 1, y, -z + 3/2]

Table S6 Comparison of the decay life time data of title compounds and the reported ones.

Compounds	(λexc, λem)	Decay times (average)	Ref
$(BZA)_2PbBr_4$	320, 406/426	0.71	[7]
$Ea_4Pb_3Cl_{10}$	375, 500	1.77	[8]
Epz $PbBr_4$	330, 596	2.7	[9]
$MAPbI_3$	470, 550	2.85	[10]
$(HA)_2(MA)_2Pb_3I_{10}$	470, 600	3.61	[10]
$(BZA)_2PbBr_{0.5}Cl_{3.5}$	320, 406/500	4.17	[7]
1	450, 605	5.97	This work
2	450, 587	6.23	This work

Table S7 The comparison of proton conductivities of the title compounds and the reported related crystalline materials

Compound	Measurement conditions	σ(S cm^{-1})	Ref
$\{[Co_3(p\text{-}ClPnHIDC)_3(H_2O)_3]\cdot 6H_2O\}_n$	100 °C, 93%RH	1.47×10^{-4}	[11]
[Triethylpropylammonium][PbI_3]	200 °C, 0% RH	4.47×10^{-5}	[12]
$\{[Co_3(m\text{-}ClPhIDC)_2(H_2O)_6]\cdot 2H_2O\}_n$	100 °C, 98%RH	7.62×10^{-4}	[11]
$[C_5H_9NH_3]_4CdBr_6$	100°C, 0%RH	4.23×10^{-7}	[13]
$(C_6H_{13}N)_2BiI_5$	140°C, 0%RH	4.18×10^{-6}	[14]
$Zn(H_2PO_4)_2(124triH)_2$	150°C, 0%RH	1.2×10^{-4}	[15]
$(Mo_5P_2O_{23})[Cu(phen)(H_2O)]_{33}\ 5H_2O$	28°C, 98%RH	2.2×10^{-5}	[16]
1	95°C, 90%RH	2.27×10^{-4}	This work
2	95°C, 90%RH	2.09×10^{-4}	This work

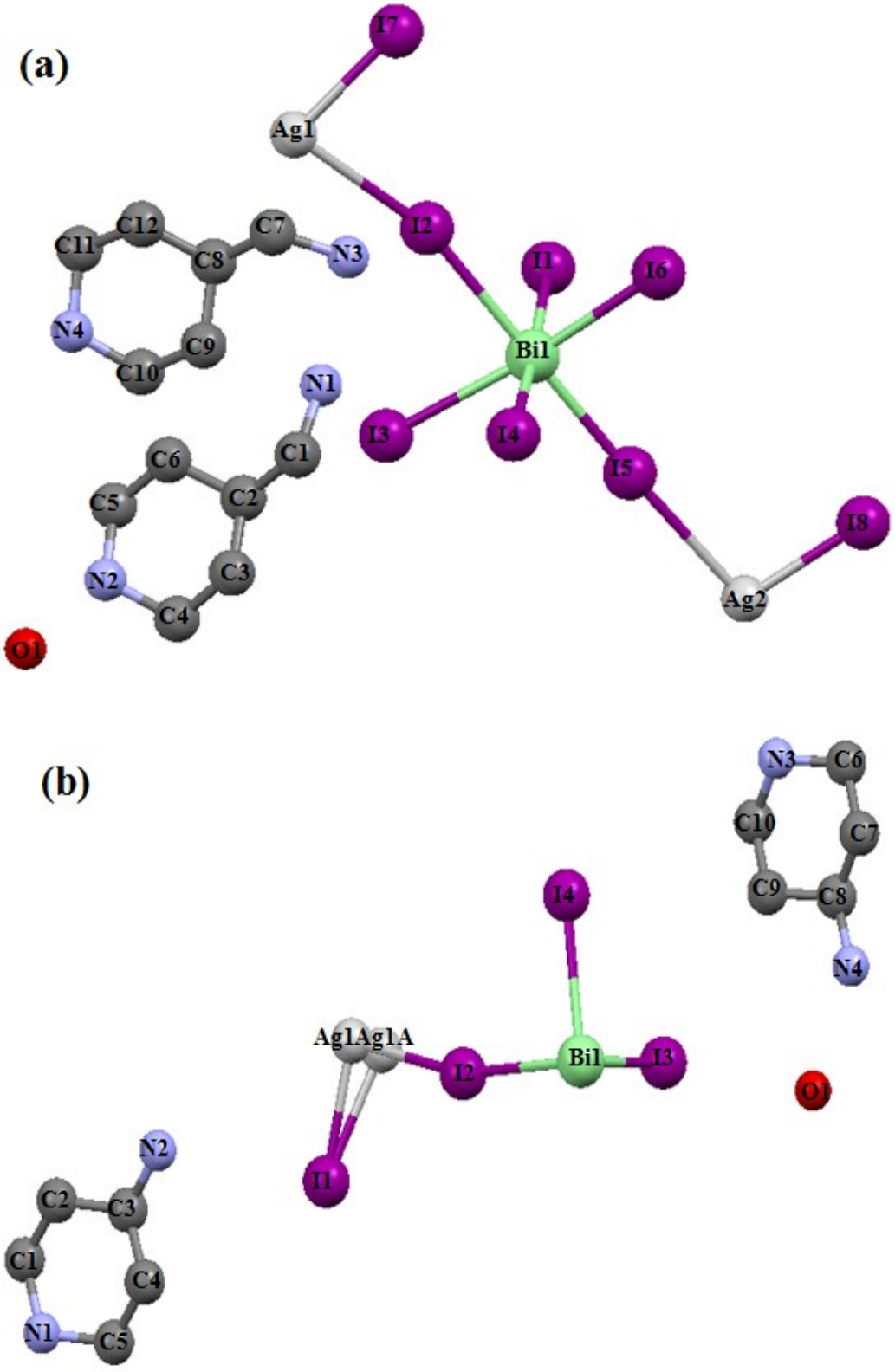

Figure S1. (a) Assymetric unit of **1**. (b) Assymetric unit of **2** (hydrogen atoms are omitted for the clarification).

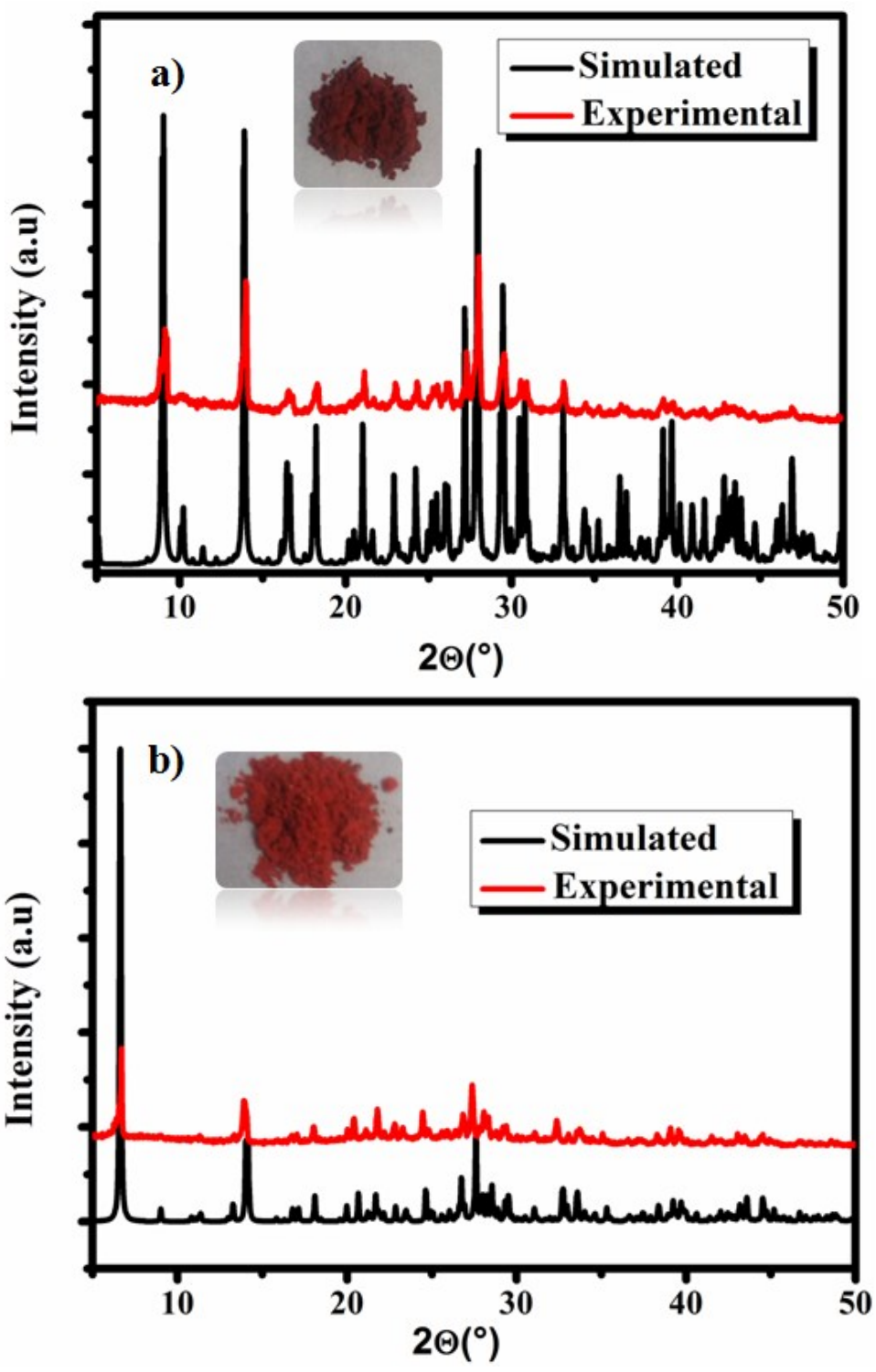

Figure S2. (a) Powder XRD patterns of **1**. Inset: photograph of the Powder. (b) Powder XRD patterns of **2**. Inset: photograph of the Powder.

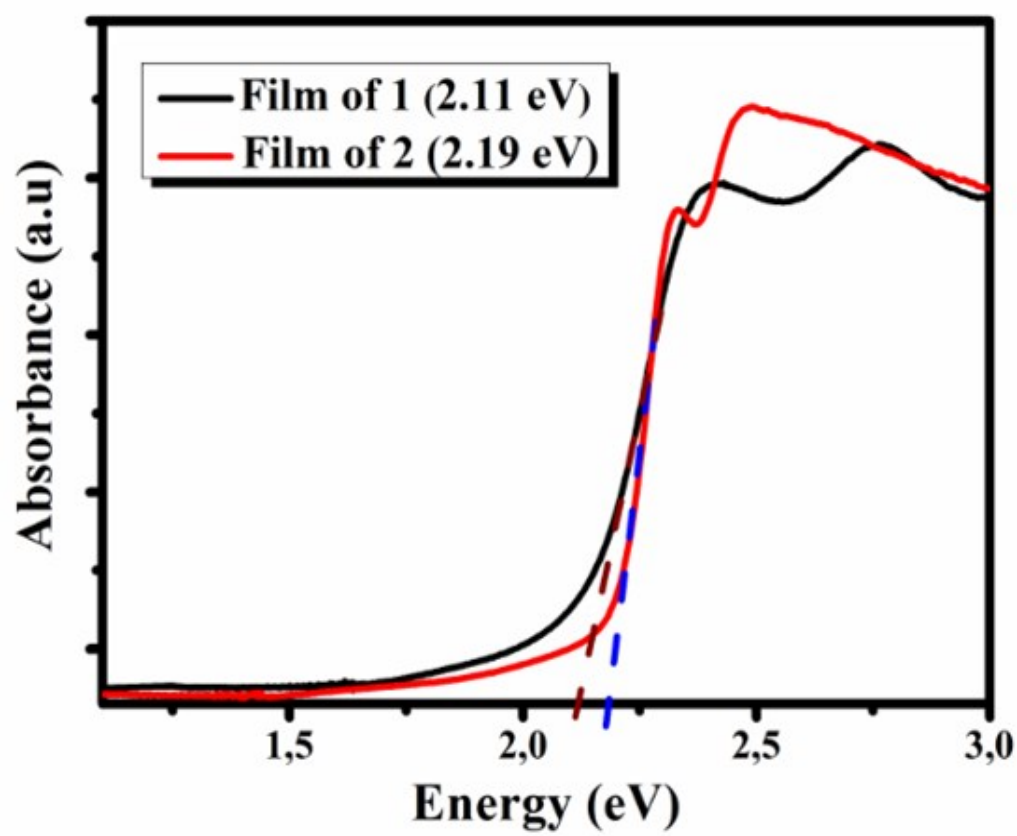

Figure S3. (a) Absorption spectra for film **1** and **2**.

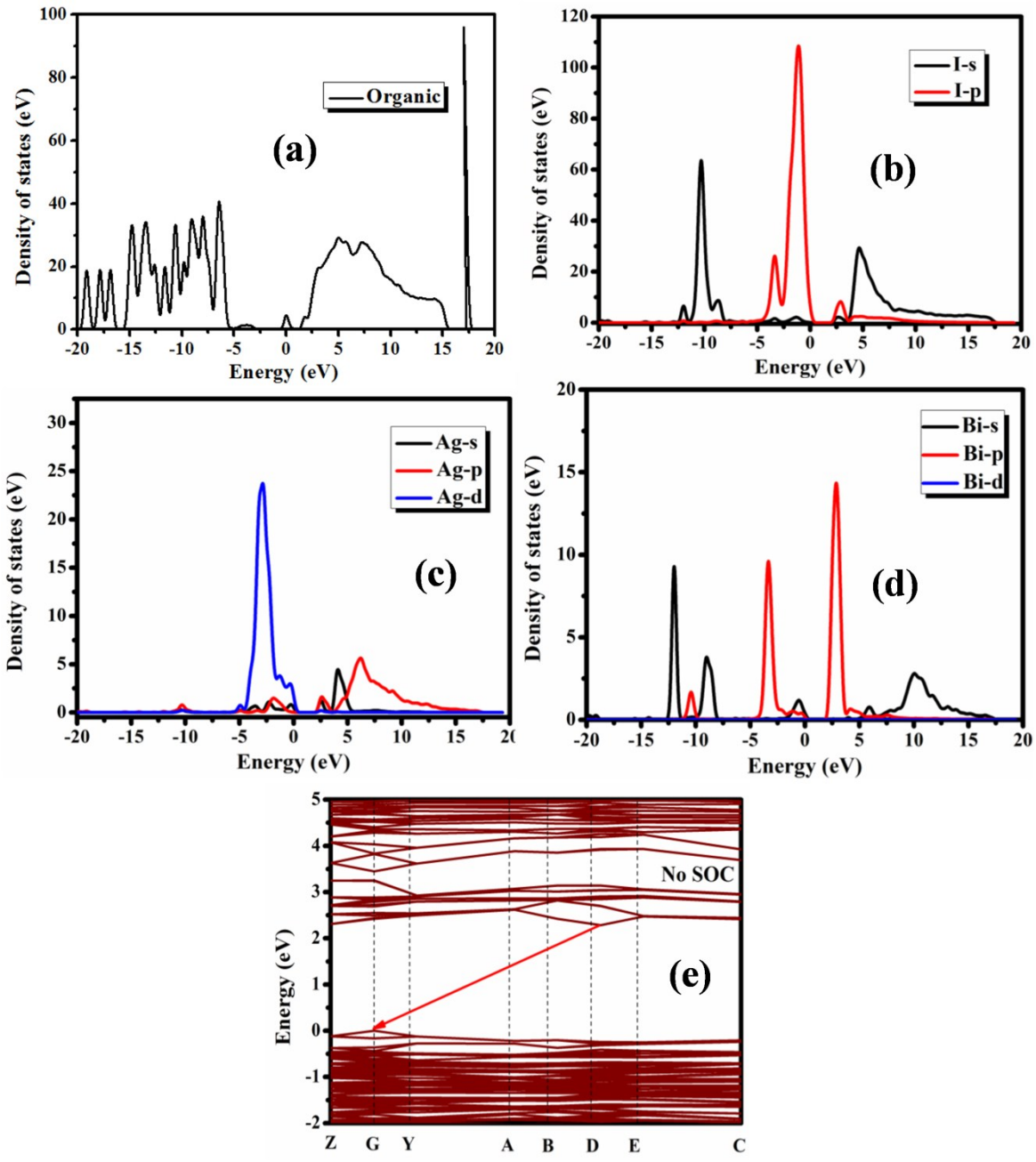

Figure S4. (a-d) Partial density of states (PDOS) of compound **1** (organic part, I-s, I-p, Ag-s, Ag-p, Ag-d, Bi-s, Bi-p and Bi-d). (e) The band structure of **AgBiI** without SOC.

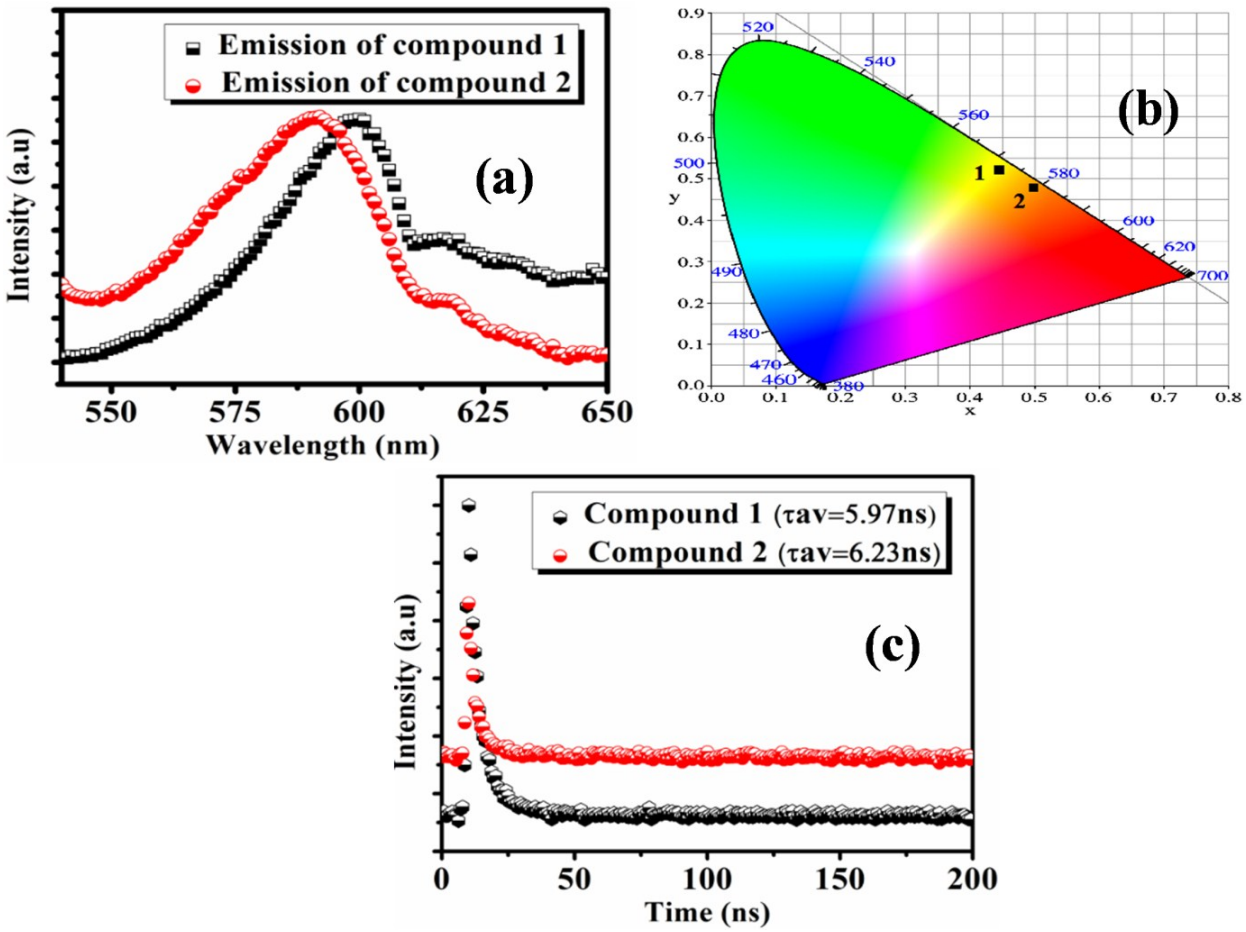

Figure S5. (a) The steady-state room-temperature photoluminescence (PL) spectra of **1** and **2**. (b) CIE1931 diagram chromatic coordinates of **1** and **2** upon 450 nm excitation. (c) The fluorescence decay time spectrum of compound **1** and **2**.

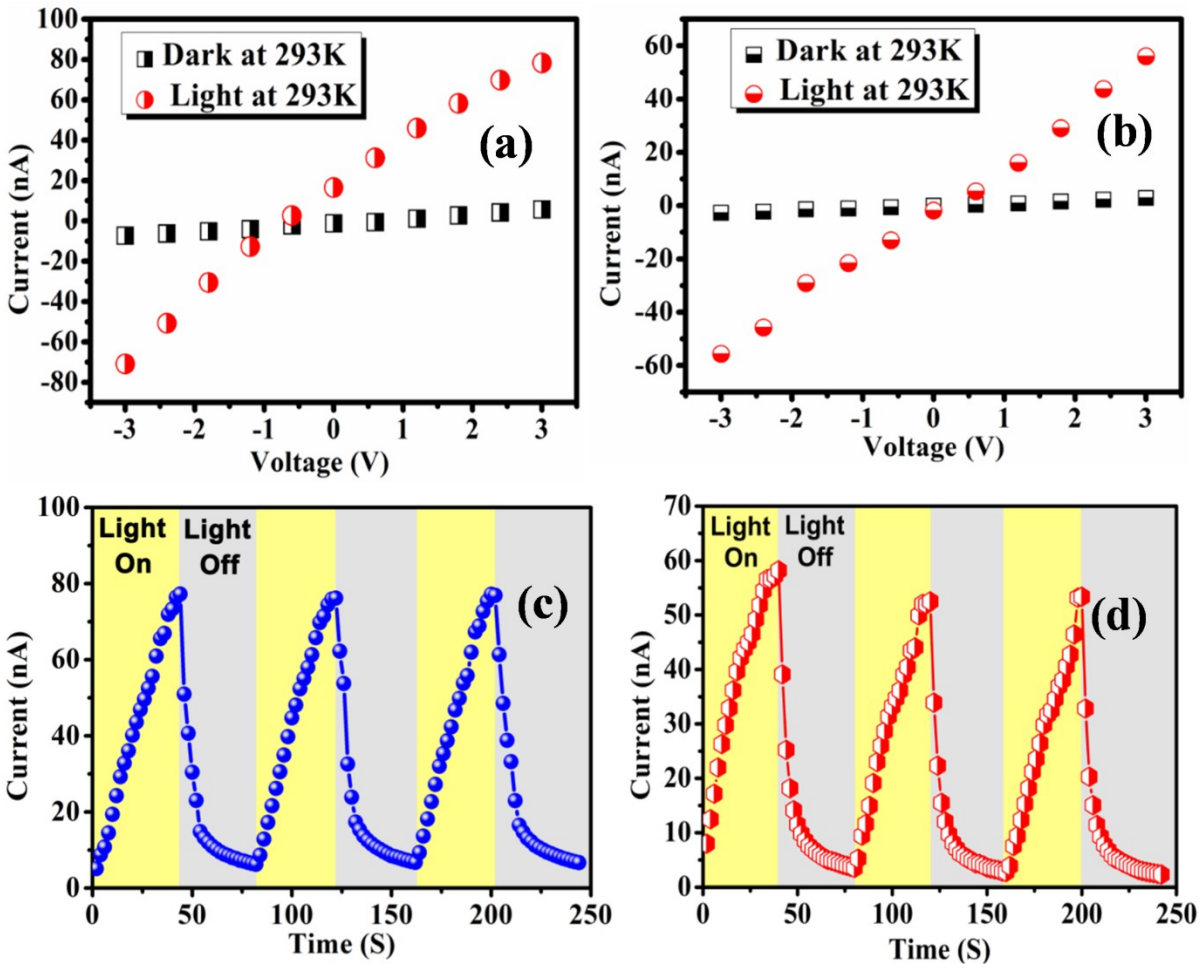

Figure S6. (a, b) I–V plots for dark and light current of **1** (a) and **2** (b) measured at 293 K under a 350 W Xenon lamp. (c, d) I–t plots of several irradiation cycles of **1** (c) and **2** (d).

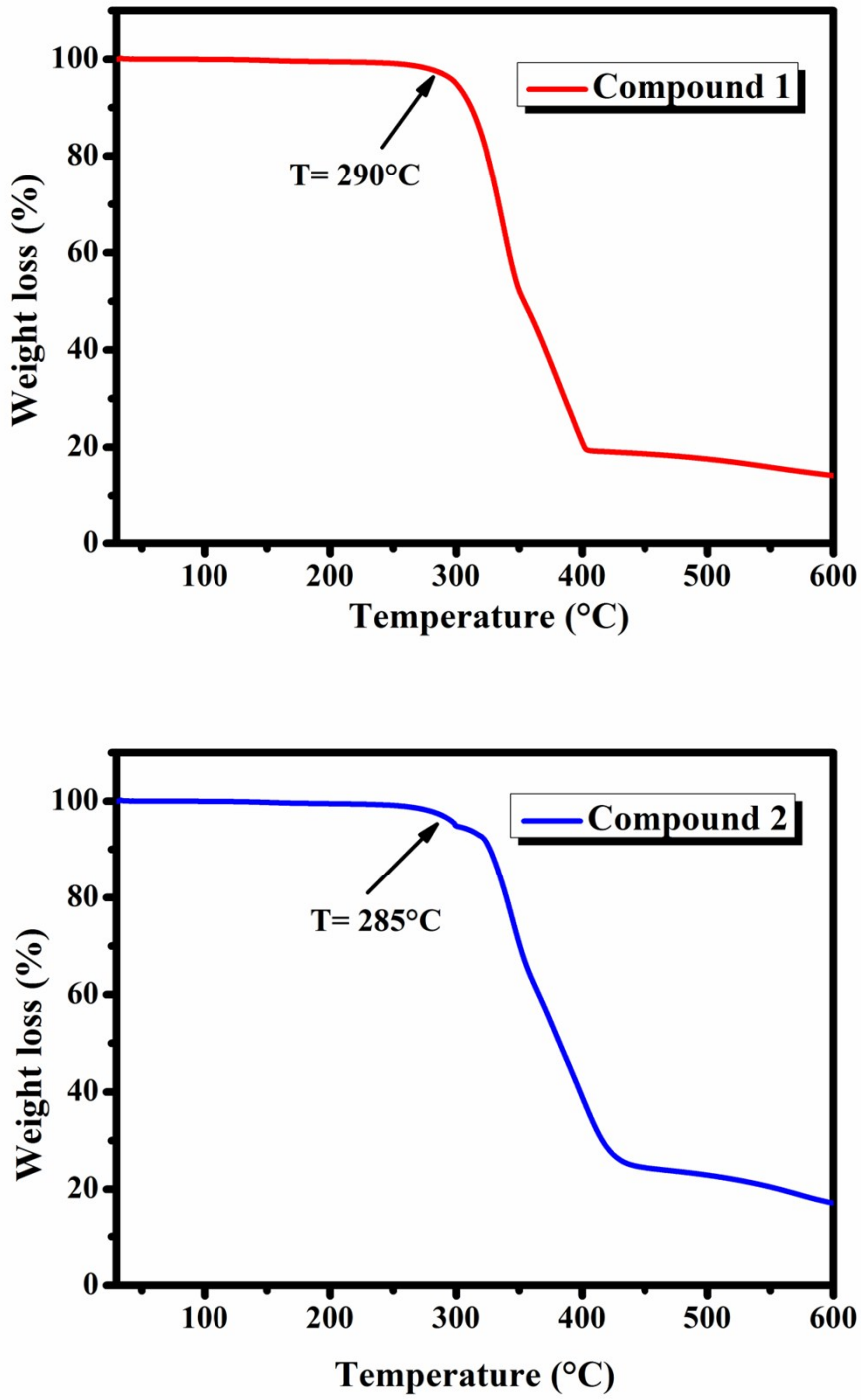

Figure S7. TGA curves of **1** and **2**

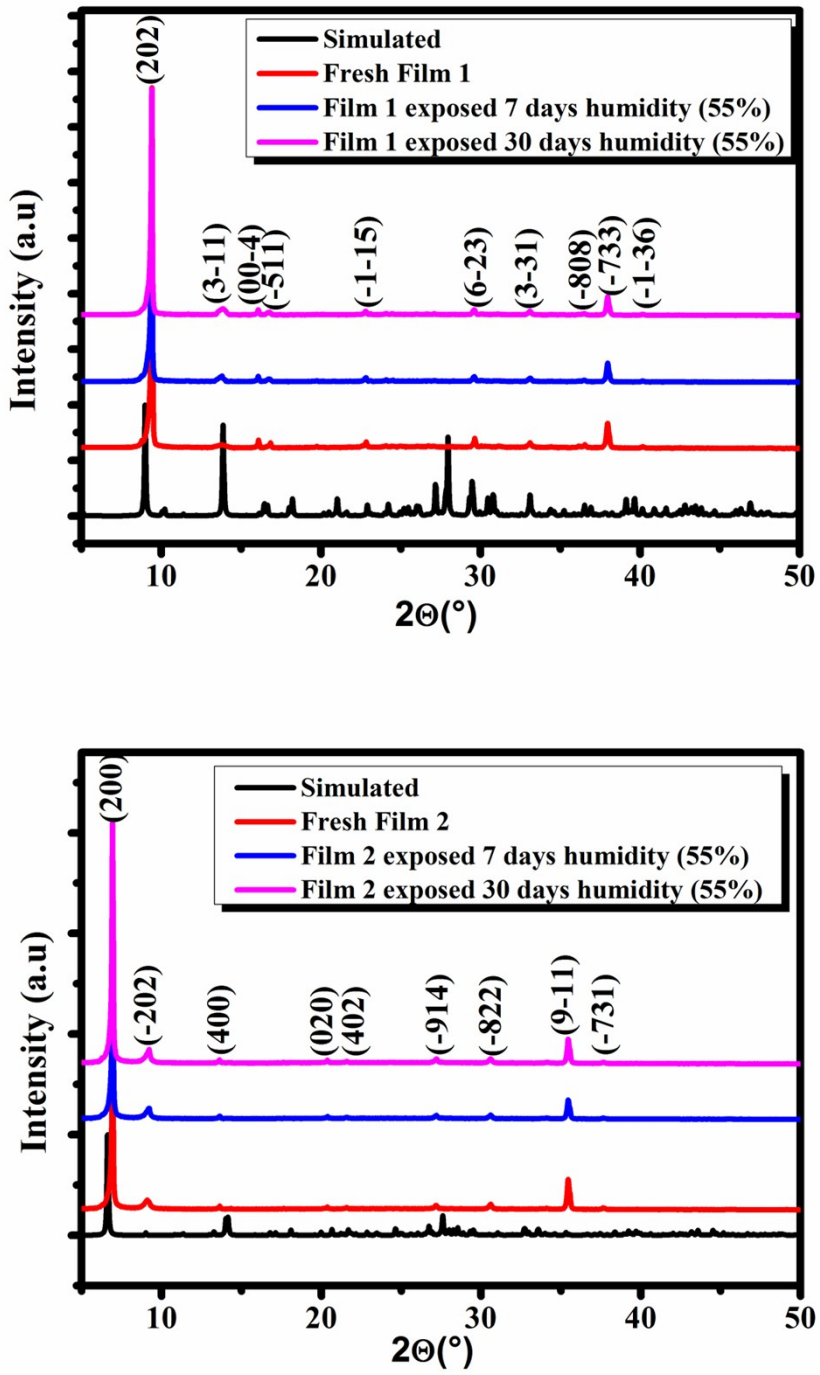

Figure S8. Stability of **1** and **2** towards humidity showing XRD Thin Films of **1** and **2** before and after exposure to 55% relative humidity and 25 ºC at different times.

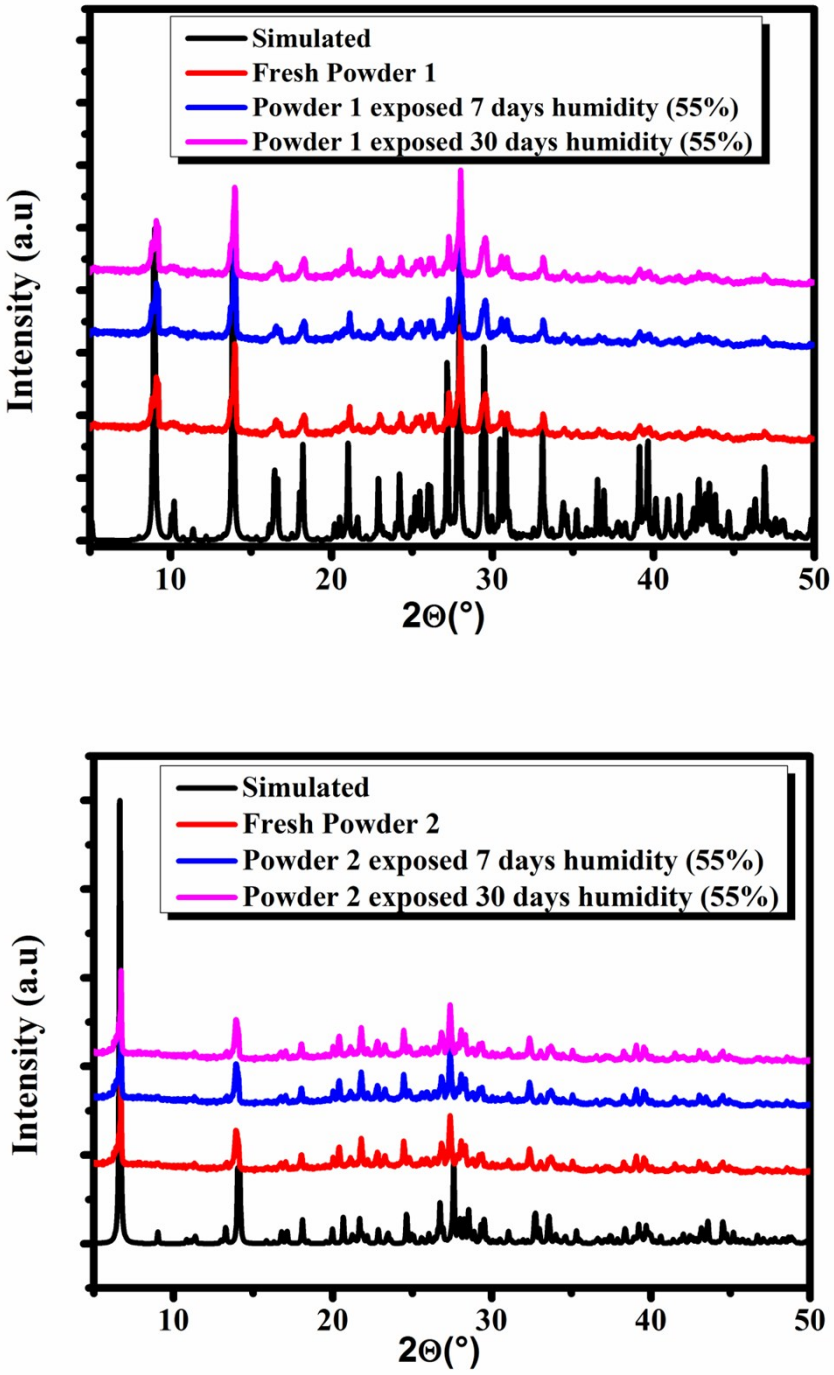

Figure S9. Stability of **1** and **2** towards humidity showing PXRD of **1** and **2** before and after exposure to 55% relative humidity and 25 ºC at different times

References :

[1] G. M. Sheldrick, Acta Crystallogr. A., ***2008***, 64, 112-122.
[2] M. C. Payne, M. P. Teter, D. C. Allan, T. A. Arias, J. D. Joannopoulos, Rev. Mod. Phys., ***1992***, 64, 1045-1097.
[3] S. J. Clark, M. D. Segall, C. J. Pickard, P. J. Hasnip, M. J. Probert, K. Refson, M. C. Payne, Z. Kristallogr. - Cryst. Mater., ***2005***, 220, 567-667.
[4] J.P. Perdew, A. Zunger, Phys. Rev. B. **1981**, *23*, 5048–5079.
[5] A. M. Rappe, K. M. Rabe, E. Kaxiras, J. D. Joannopoulos, Phys. Rev. B: Condens. Matter Mater. Phys., ***1990***, 41, 1227-1230.
[6] L. Kleinman, D. M. Bylander, Phys. Rev. Lett. ***1982***, 48, 1425-1428.
[7] M-H. Jung, Inorg. Chem. ***2019***, 58, 6748−6757.
[8] L. Mao, Y. Wu, C. C. Stoumpos, B. Traore, C. Katan, J. Even, M. R. Wasielewski, and M. G. Kanatzidis, J. Am. Chem. Soc., ***2017***, 139, 11956−11963.
[9] L, Mao, P. Guo, M. Kepenekian, I. Hadar, C. Katan, J. acky Even, R. D. Schaller, C.C. Stoumpos, and M.G. Kanatzidis, J. Am. Chem. Soc., ***2018***, 140, 13078−13088.
[10] Jung, H. Mi-Hee, J. Mater. Chem. A., ***2019***, 7,14689.
[11] X. Liang , B. Li , M. H. Wang , J. Wang , R. L. Liu, and G. Li , *ACS Appl.* Mater. Interfaces., ***2017***, 9 , 25082 -25086.
[12] M. J. Wang , X. R. Chen , Y. B. Tong , G. J. Yuan , X. M. Ren, and J. L. Liu , Inorg. Chem., **2017**, 56, 9525 -9534
[13] S. Wang, L. Li, Z. Sun, C. Ji, S. Liu, Z. Wu, S. Zhao, A. Zeb, M. Hong, and J. Luo, J. Mater. Chem. C., ***2017***, 5, 4731-4735.
[14] W. Zhang, K. Tao, C. Ji, Z. Sun, S. Han, J. Zhang, Z. Wu, and J. Luo, Inorg. Chem., ***2018***, 578, 4239-4243.
[15] D. Umeyama, S. Horike, M. Inukai, T. Itakura, S. Kitagawa, J. Am. Chem. Soc., ***2012***, 134, 12780–12785.
[16] C. Dey, T. Kundu, R. Banerjee, Chem. Commun., ***2012***, 48, 266–268.